

DENDRITIC CELL BASED IMMUNOTHERAPY FOR MELANOMA

KUN DONG

University of California, Los Angeles

BINAN GU

University of Southern California

LUCY ODOM

California State University, Fullerton

APARNA SARKAR

Pomona College

ADVISOR: CYMRA HASKELL

University of Southern California

August 10, 2012

Abstract

Dendritic cells (DC) are important immunostimulatory cells that facilitate antigen transport to lymphoid tissues and provide stimulation of cytotoxic T lymphocyte (CTL) cells. In this paper, we attempt to understand the details of the regulation and kinetics of the DC-CTL interaction in the DC-based immunotherapeutic treatment of human melanoma cancer. We study a previously defined model, which integrates dendritic cell populations in the blood, spleen, and the tumor. Ultimately, we are interested in applying analysis of the model towards higher rates of efficacy of DC treatment.

1 Introduction

Dendritic cell treatment is a recently developed immunotherapy for cancer. Immunotherapies boost a patient's immune response to a pathogen by administering vaccinations or introducing antibodies. In the case of dendritic cell therapy, the vaccination consists of dendritic cells.

Dendritic cells (DCs) act as messengers between a specific pathogen and cytotoxic T-lymphocytes (CTLs), which are the fighter cells of the immune system. After encountering a tumor, DCs travel to the lymphoid organs and present the tumor-specific antigen to naive CTLs. The naive CTLs then either develop into activated CTLs or memory CTLs. The activated CTLs travel to the tumor site and fight the pathogen, killing tumor cells via apoptosis. Memory CTLs circulate in the blood and lymphoid organs, prepared for a future attack on the body by the same pathogen.

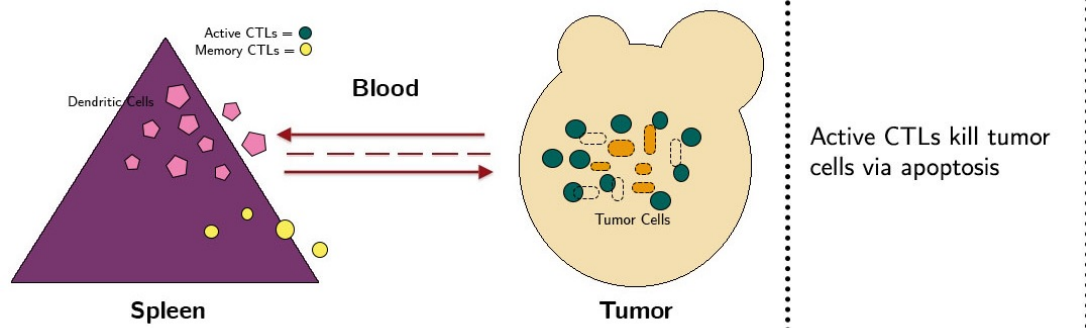
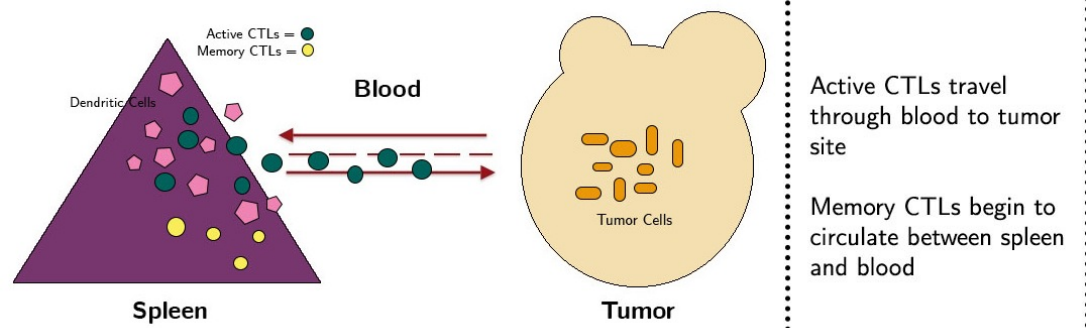
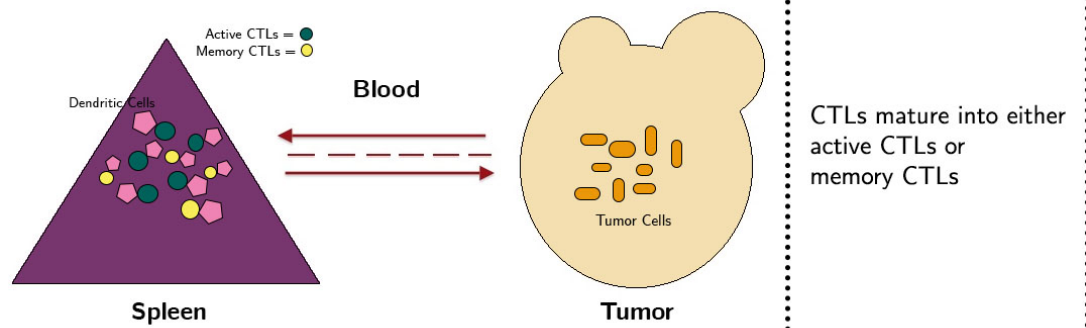
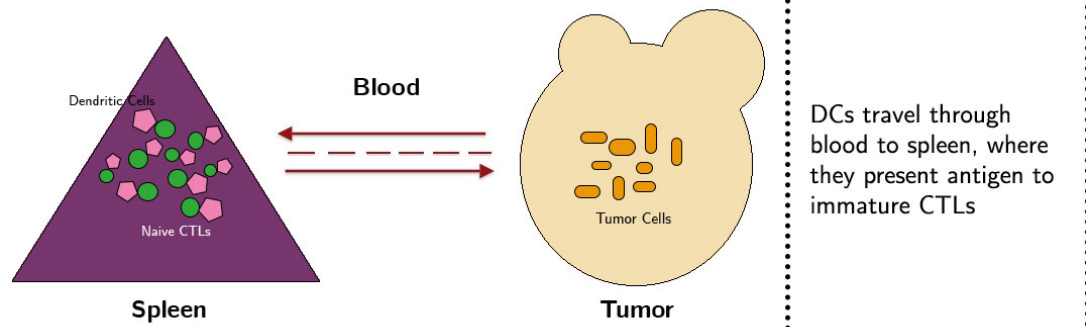
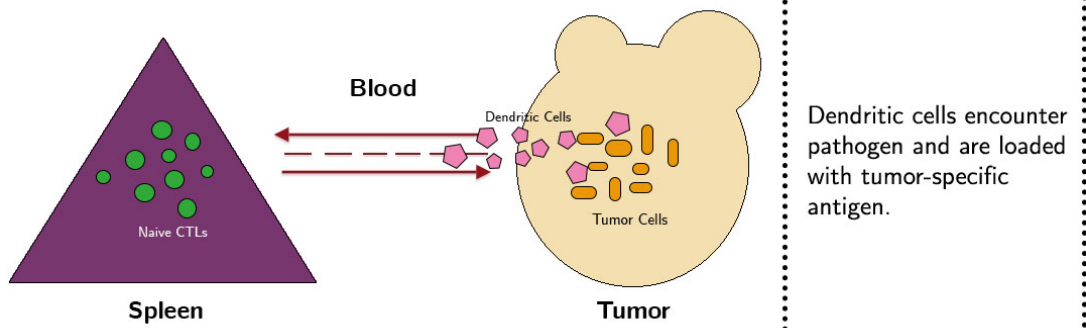
Previous biological studies have demonstrated the efficacy of dendritic cell treatment on field mice. In these clinical trials, researchers cultivate a subject's immature DCs ex

vivo and load them with tumor-specific antigens. This culture is used as a patient-specific vaccine, injected to boost the native response against tumor cells. Success of these studies has led to FDA approval of the first dendritic cell vaccine for prostate cancer. However, it has proven difficult to predict how different patients will react to DC treatment. In this paper we are concerned with analyzing a mathematical model of the immune response with DC treatment in order to determine an optimal treatment regimen and to understand how this might vary from patient to patient.

Ludewig *et al.* presented results from murine experiments of DC treatment in the form of data and a mathematical model of DC-CTL interactions. In their experiments, mice received injections of melanoma-specific DCs. No tumor was present in their bodies. So, the resulting model is one of DC trafficking in the body—specifically in the lung, liver, spleen, and blood. DePillis *et al.* modified and extended Ludewig *et al.*'s model by combining all the lymphoid organs into a single compartment which they call the spleen and by including a tumor compartment. The result is a model of the immune response to DC treatment in the presence of a tumor, allowing for analysis of varying DC treatments in terms of tumor growth and patients' particular parameter values. The values we have used in our analysis are those estimated by DePillis *et al.* to fit experimental data from Ludewig *et al.*

2 The Model

We are studying DC trafficking and immune activity between the spleen and the tumor via the blood. Dendritic cells and active CTLs move between both the spleen and the tumor, while memory CTLs do not travel to the tumor (remaining in the blood and spleen in case of future attack). The following diagrams explain the body's native immune response to a tumor.



The model developed by DePillis *et al.* [2] is a compartment model involving three compartments: the blood, spleen, and tumor. It involves nine state variables and boils down to a system of nine first order non-linear differential equations. The variables are:

D_{blood}	Number of dendritic cells in the blood;
D_{spleen}	Number of dendritic cells in the spleen;
E_{blood}^a	Number of activated CTLs in the blood;
E_{spleen}^a	Number of activated CTLs in the spleen;
E_{blood}^m	Number of memory CTLs in the blood;
E_{spleen}^m	Number of memory CTLs in the spleen;
E_{tumor}^a	Number of activated CTLs in the tumor;
T	Number of tumor cells;
D_{tumor}	Number of melanoma infiltrating dendritic cells (MIDCs).

Notice that the model tracks four different types of cells: dendritic cells, activated CTLs, memory CTLs, and tumor cells. Most of the terms in the equations model death of the cells or their migration from one organ to another. These terms all follow the pattern of a rate coefficient multiplying a variable; the first two terms in Equation (1) are two simple examples. Some of the percentage rates of change are not constant but depend on other variables, as in the first term in Equation (2). Other terms represent the growth or production of cells and the injection of DCs through vaccination. We will examine each compartment and equation separately (see Table 1 in the Appendix for a complete list of parameters).

Blood Compartment

$$\frac{d}{dt}D_{blood} = -\mu_B D_{blood} + \mu_{TB} D_{tumor} + v_{blood}(t) \quad (1)$$

$$\frac{d}{dt}E_{blood}^a = \mu_{SB}(D_{spleen})E_{spleen}^a - \mu_{BB}E_{blood}^a \quad (2)$$

$$\frac{d}{dt}E_{blood}^m = \mu_{SB}(D_{spleen})E_{spleen}^m - \mu_{BB}E_{blood}^m \quad (3)$$

Equation (1) provides a good example of the general pattern of the model. The first term models the number of DCs leaving the blood and traveling to all lymphoid organs in the body. This includes the spleen, so jumping ahead to (4), we see how the DC transfer rate from blood to spleen (μ_{BS}) is a small portion of the emigration rate of DCs out of the blood (μ_B). Our second term is a straight trafficking term, modeling the transfer of DCs from tumor to blood. This term corresponds to the second term in (9). The last term of (1) indicates the therapeutic injection of dendritic cells into the blood. This term is typically piecewise constant.

The first term in Equation (2) is a trafficking term indicating the migration of active CTLs from spleen to blood. It corresponds to the second term in Equation (5). However, we see that the percentage rate at which these cells move from the spleen is a function that

depends on D_{spleen} :

$$\mu_{SB}(D_{spleen}) = \mu_{SB}^* + \frac{\Delta\mu}{1 + \frac{D_{spleen}}{\theta_{shut}}}$$

where $\Delta\mu = \mu_{SB}^{Normal} - \mu_{SB}^*$

This term comes from Ludwig *et al.* and models the empirical observation that active CTLs are held back in the spleen when there are a large number of DCs there. The graph of $\mu_{SB}(D_{spleen})$ is shown in Figure 1. Notice that it drops very rapidly and is essentially equal to μ_{SB}^* for any value of D_{spleen} more than about 50. The second term models the

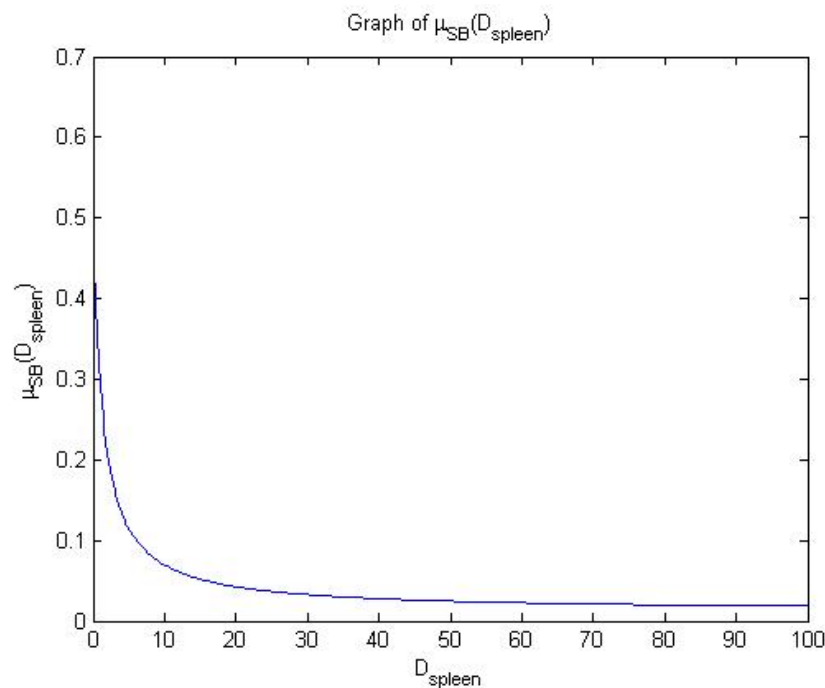


Figure 1: The percentage rate at which active CTLs migrate from the spleen to the blood is close to μ_{SB}^{Normal} when D_{spleen} is very small but decays rapidly to μ_{SB}^* as D_{spleen} increases.

migration of active CTLs out of the blood, traveling to **all** other parts of the body among which are the spleen and tumor. This term corresponds to the first terms in Equation (5) and (7) where we notice that $\mu_{BTE}(T) < \mu_{BB}$ for all T , so $\mu_{BSE} + \mu_{BTE}(T) < \mu_{BB}$.

Equation (3) follows equation (2), with memory CTLs substituted for active CTLs; biologically, in fluctuation between spleen and blood, active and memory cells are treated the same.

Spleen Compartment

$$\frac{d}{dt}D_{spleen} = \left(MaxD(1 - e^{\frac{-\mu_{BS}D_{blood}}{MaxD}}) \right) - a_D D_{spleen} - b_{DE} E_{spleen}^a D_{spleen} \quad (4)$$

$$\begin{aligned} \frac{d}{dt}E_{spleen}^a = & \mu_{BSE} E_{blood}^a - \mu_{SB}(D_{spleen}) E_{spleen}^a + b_a D_{spleen} E_{spleen}^m \\ & - a_{EaS} E_{spleen}^a + a_{EaS} DC_{on}(D_{spleen}) E_{naive} - r_{am} E_{spleen}^a \\ & + b_p \frac{D_{spleen}(t - \tau_D) E_{spleen}^a(t - \tau_D)}{\theta_D + D_{spleen}(t - \tau_D)} \end{aligned} \quad (5)$$

$$\begin{aligned} \frac{d}{dt}E_{spleen}^m = & r_{am} E_{spleen}^a - a_{Em} E_{spleen}^m - b_a D_{spleen} E_{spleen}^m - \mu_{SB}(D_{spleen}) E_{spleen}^m \\ & + \mu_{BSE} E_{blood}^m \end{aligned} \quad (6)$$

The first term of Equation (4) models the migration of dendritic cells in the blood to the spleen. It stands out as the only migration term in the model that is written as a the transfer rate of DCs from the blood to the spleen, instead of as a percentage rate multiplied by D_{blood} . The graph of this term is shown in Figure 2. The term is a modification of the

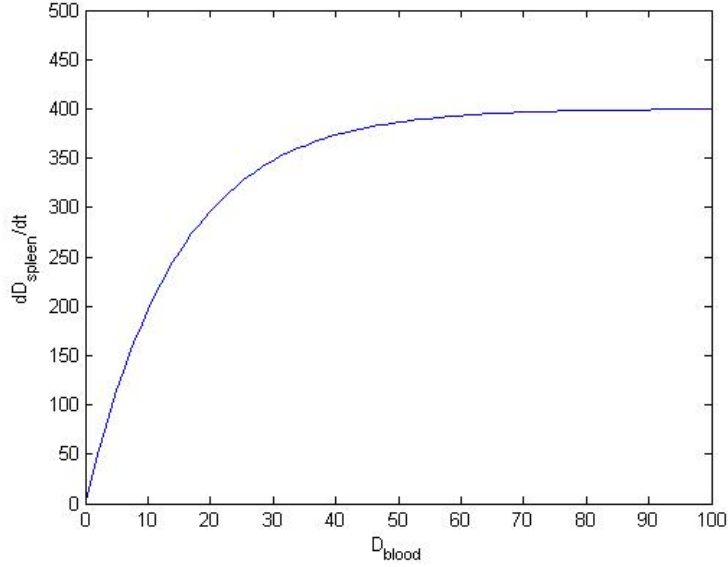


Figure 2: When D_{blood} is close to 0, the transfer rate of DCs from blood to spleen is close to μ_{BS} . When D_{blood} is large, the actual rate (and not the percentage rate) is close to $MaxD$ (this means the percentage rate tends to 0 as $D_{blood} \rightarrow \infty$).

Ludewig *et al.* model by DePillis *et al.*, accounting for the existence of a maximum rate at which DCs enter the spleen [2]. Through model simulation and fit to experimental data, DePillis *et al.* found this rate to be limited to about 400 cells per day: $MaxD = 400$ [2]. Notice that the *percentage* rate at which DCs enter the spleen from the blood is

$$\frac{MaxD(1 - e^{\frac{-\mu_{BS}D_{blood}}{MaxD}})}{D_{blood}} < \mu_{BS}.$$

As mentioned in the explanation of the first term in Equation (1), $\mu_{BS} < \mu_B$ because that term also includes migration of DCs into other organs of the body. The second term of Equation (4) models the death of dendritic cells in the spleen. When dendritic cells meet active CTLs in the spleen they are consumed enabling the proliferation of more active CTLs. The third term in Equation (4) models this and it corresponds to the last term in Equation (5).

Equation (5) has many components, including two new and exciting terms. It begins with the migration of active CTLs from blood to spleen, which we previously discussed in Equation (2). Similarly, the second term is a trafficking term modeling the migration of active CTLs from spleen to blood and corresponds to the second term in Equation 2. The third term is another trafficking term, modeling the conversion of memory CTLs to active CTLs in the presence of DCs. It corresponds to the third term in Equation (6). Moving to the second line, the fourth term models the death of active CTLs in the spleen. The fifth term models the conversion of naive CTLs to active CTLs in the presence of dendritic cells. Note that E_{naive} is the number of naive CTLs in the spleen—a constant in this model and not a variable. The function DC_{on} is a step function:

$$DC_{on}(D_{spleen}) = \begin{cases} 0 & \text{if } D_{spleen} = 0 \\ 1 & \text{if } D_{spleen} > 0 \end{cases}$$

DePillis *et al.* introduced $DC_{on}(D_{spleen})$ to prevent the creation of tumor-specific CTLs before there are any DCs to present the antigen to the naive T-cells. We find it a little strange that the coefficient in this term, $a_{E_3^a}$, is the same as the percentage rate at which active CTLs die; this assumption seems tenuous at the moment, meriting further exploration and potential modification. However, we don't expect any modification to yield substantive differences in our analysis, so for now we have accepted that the rates are the same. Just as DCs cause some memory CTLs to activate, some activated CTLs revert to memory CTLs. This reversion from active to memory CTLs is modeled by the sixth term in the equation. It is a trafficking term, so we see it again as the first term of Equation (6).

The final term of (5) incorporates a time delay, which presents considerable challenges in the analysis. Biologically, the delay represents the time that DCs and naive CTLs in the spleen need to be in contact before proliferation of active CTLs begins [2]. Accordingly, this last term models the proliferation of more active CTLs from some active CTLs. Recall from Equation (4) that active CTLs kill some DCs in the spleen in order to proliferate. The percentage rate of proliferation is equal to

$$b_p \frac{D_{spleen}(t - \tau_D)}{\theta_D + D_{spleen}(t - \tau_D)}.$$

When $D_{spleen}(t - \tau_D) = 0$ there is no proliferation. As $D_{spleen}(t - \tau_D)$ increases the percentage rate of proliferation increases with a limiting value of b_p .

Moving on to equation (6), we first observe the reversion of active CTLs to memory CTLs. The second term models the natural death of memory CTLs in the spleen. With its counterpart back in Equation (5), the third term models the activation of memory CTLs by DCs. The fourth term is familiar—memory cells are transferred from spleen to blood in the same way that active cells are (as seen in Equation (5))—and its counterpart is the first

term in Equation 3. The last terms models the migration of memory CTLs from the blood to the spleen and its counterpart is the second term in Equation 3.

Tumor Compartment

$$\frac{d}{dt}E_{tumor}^a = \mu_{BTE}(T)E_{blood}^a - a_{E_a T}E_{tumor}^a - cE_{tumor}^a T \quad (7)$$

$$\frac{d}{dt}T = rT \left(1 - \frac{T}{k}\right) - \mathcal{D}(E_{tumor}^a, T)T \quad (8)$$

$$\frac{d}{dt}D_{tumor} = \frac{mT}{q + T} - \mu_{TB}D_{tumor} - a_D D_{tumor} + v_{tumor}(t) \quad (9)$$

where

$$\begin{aligned} \mu_{BTE}(T) &= \mu_{BB} \frac{T}{\alpha + T} \\ \text{and} \quad \mathcal{D}(E_{tumor}^a, T) &= d \frac{\left(\frac{E_{tumor}^a}{T}\right)^l}{s + \left(\frac{E_{tumor}^a}{T}\right)^l} \end{aligned} \quad (10)$$

We jump right into (7). The first term models the migration of active CTLs in the blood to the tumor. The rate function $\mu_{BTE}(T)$ can be understood as the a fraction of the total elimination of CTLs from the blood, which increases as the number of tumor cells increases. So when there are more tumor cells, a greater proportion of the active CTLs leaving the blood will go to the tumor instead of traveling to other organs. As previously noted in our discussion of the blood compartment, this term corresponds to a portion of emigration of active CTLs from the blood in equation (2):

$$\mu_{BB} \frac{T}{\alpha + T} < \mu_{BB}.$$

The second term models the natural death of active CTLs in the tumor. The third term models the inactivation of active CTLs by tumor cells; think of this as the tumor's combat of the immune system's fighter cells.

The two terms of equation (8), the rate of change in number of tumor cells, are a growth term and a decay term respectively. The growth term represents logistic growth, as used in previous models and fit to experimental data [2]. The percentage rate at which tumor cells grow is equal to the parameter r when T is small and decreases to 0 as T increases. The percentage rate at which active CTLs kill tumor cells, \mathcal{D} , depends on the "kill ratio" of active CTLs in the tumor to tumor cells. Its graph is shown in Figure 3. This rate is equal to 0 when there are no active CTLs and increases up to a maximum of d as the kill ratio increases. Notice that \mathcal{D} is not continuous when $E_{tumor}^a = T = 0$, so this term is not differentiable in this 7-dimensional subspace of phase space.

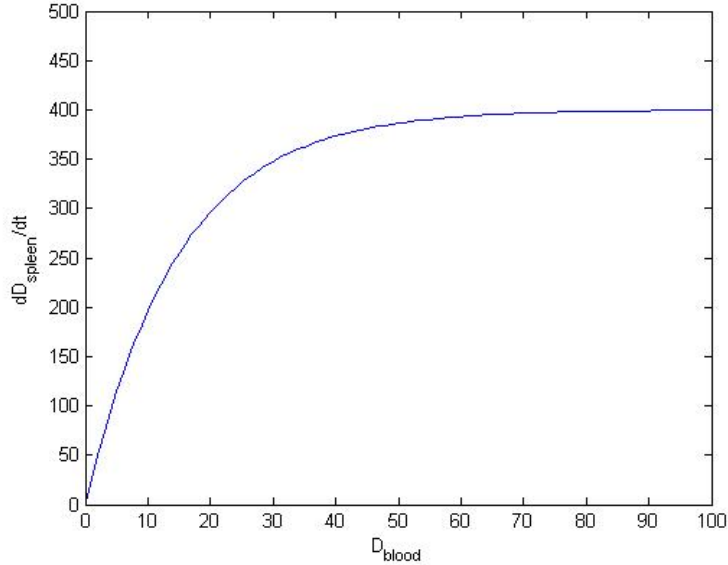


Figure 3: \mathcal{D} is the percentage rate at which tumor cells are killed off; it ranges between 0 when $\frac{E_{tumor}^a}{T}$ is small to d when $\frac{E_{tumor}^a}{T}$ is large.

The first term in Equation (9) models the migration of DCs to the tumor due to the native immune response. This rate increases as a saturation-limited function of the number of tumor cells; the model assumes that the body has an infinite supply of dendritic cells to send to the tumor site as dictated [2]. The second term accounts for DC transfer from tumor to blood as well as natural death of DCs in the tumor. The transfer term here is the negative side of the trafficking term we saw in Equation (1). The final term is another injection function, as DePillis *et al.* ran simulations with both intravenous and intratumoral DC injections.

Simulations

Simulations of the system indicate that all solutions tend to one of two equilibria. Figures 4 and 5, run for the same parameter values and different initial conditions, depict both of these equilibria.

3 Equilibria

Consider the region of the 9-dimensional space where all the variables are non-negative. It is easy to see that this region is invariant. We are only interested in solutions that live in this part of the space, since other solutions are not physically meaningful. Notice that the system is infinite-dimensional because of the delay; initial conditions consist of the values

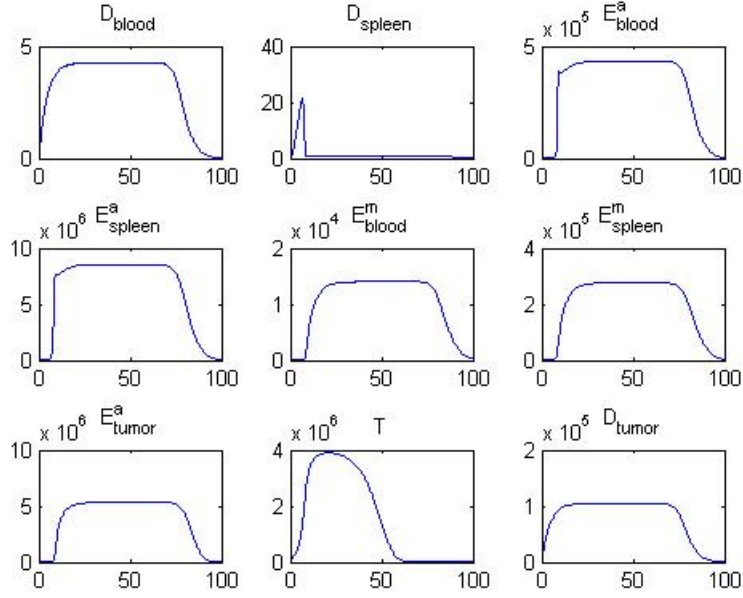


Figure 4: Initial condition: $T = 10^5$, all other variables 0

of the variables not just at $t = 0$ but at every value of t from $-\tau$ to 0. We would like to understand which initial conditions and values of the parameters will yield solutions where $T \rightarrow 0$ as $t \rightarrow \infty$. It may also be of interest to identify those initial conditions where T remains small but we have not focused on this matter in this paper. Although ultimately we would like to understand what injection regimens produce solutions where $T \rightarrow 0$, in this paper we have primarily restricted our analysis to the body's native immune response where $v_{blood}(t) \equiv v_{tumor}(t) \equiv 0$.

Notice that $DC_{on}(D_{spleen})$ is discontinuous when $D_{spleen} = 0$. This means that there could be more than one solution passing through a point in phase space where $D_{spleen} = 0$. However, of particular interest to us are solutions where $T > 0$ for some $t = t^*$. Any such solution will have $D_{spleen} > 0$ for $t \geq t^*$, so $DC_{on}(D_{spleen})$ will equal one and remain one as $t \rightarrow \infty$. For this reason, in our model analysis and simulations, we replace $DC_{on}(D_{spleen})$ with 1. Since D_{spleen} is the number of dendritic cells, it does not make sense for it to take on fractional values, so in future work it may be appropriate to replace this function with another function that is similar but continuous when $D_{spleen} = 0$. In summary, we study

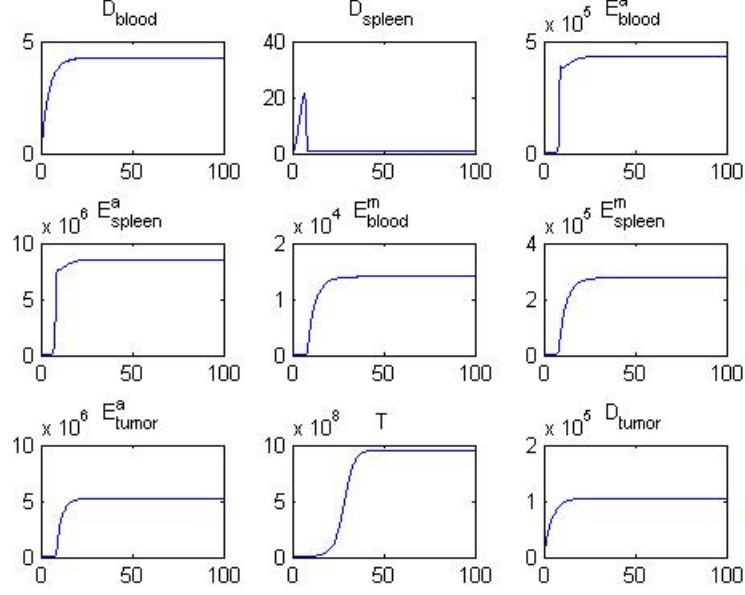


Figure 5: Initial condition: $T = 2 \times 10^5$, all other variables 0

the following system:

$$\left\{ \begin{array}{l} \frac{d}{dt} D_{blood} = -\mu_B D_{blood} + \mu_{TB} D_{tumor} \end{array} \right. \quad (11)$$

$$\left\{ \begin{array}{l} \frac{d}{dt} E_{blood}^a = \mu_{SB}(D_{spleen}) E_{spleen}^a - \mu_{BB} E_{blood}^a \end{array} \right. \quad (12)$$

$$\left\{ \begin{array}{l} \frac{d}{dt} E_{blood}^m = \mu_{SB}(D_{spleen}) E_{spleen}^m - \mu_{BB} E_{blood}^m \end{array} \right. \quad (13)$$

$$\left\{ \begin{array}{l} \frac{d}{dt} D_{spleen} = \left(MaxD(1 - e^{\frac{-\mu_{BS} D_{blood}}{MaxD}}) \right) - a_D D_{spleen} - b_{DE} E_{spleen}^a D_{spleen} \end{array} \right. \quad (14)$$

$$\left\{ \begin{array}{l} \frac{d}{dt} E_{spleen}^a = \mu_{BSE} E_{blood}^a - \mu_{SB}(D_{spleen}) E_{spleen}^a + b_a D_{spleen} E_{spleen}^m \\ \quad + a_{EaS} E_{naive} - (a_{EaS} + r_{am}) E_{spleen}^a \\ \quad + b_p \frac{D_{spleen}(t - \tau_D) E_{spleen}^a(t - \tau_D)}{\theta_D + D_{spleen}(t - \tau_D)} \end{array} \right. \quad (15)$$

$$\left\{ \begin{array}{l} \frac{d}{dt} E_{spleen}^m = r_{am} E_{spleen}^a - a_{Em} E_{spleen}^m + b_a D_{spleen} E_{spleen}^m \\ \quad + \mu_{SB}(D_{spleen}) E_{spleen}^m + \mu_{BSE} E_{blood}^m \end{array} \right. \quad (16)$$

$$\left\{ \begin{array}{l} \frac{d}{dt} E_{tumor}^a = \mu_{BTE}(T) E_{blood}^a - a_{EaT} E_{tumor}^a - c E_{tumor}^a T \end{array} \right. \quad (17)$$

$$\left\{ \begin{array}{l} \frac{d}{dt} T = \left[r \left(1 - \frac{T}{k} \right) - \mathcal{D}(E_{tumor}^a, T) \right] T \end{array} \right. \quad (18)$$

$$\left\{ \begin{array}{l} \frac{d}{dt} D_{tumor} = \frac{mT}{q + T} - (\mu_{TB} + a_D) D_{tumor} \end{array} \right. \quad (19)$$

We have primarily studied this system when the values of the parameters are those that are given in the appendix. However, since we expect the parameters to vary from individual to individual and we certainly expect the values of the parameters to be different for people than they are for mice, we are interested in how the behavior of the solutions depends on the parameters. In particular, we have noticed that the behavior of the solutions is sensitive to the relative sizes of d and r .

DePillis *et al.* have found the equilibria of the system. We reproduce their work here for completeness. To determine the equilibria we set the left hand side of equations (11)-(19) equal to zero. From equation (18) we see that either $T = 0$ or

$$r \left(1 - \frac{T}{k}\right) = d \frac{\left(\frac{E_{tumor}^a}{T}\right)^l}{s + \left(\frac{E_{tumor}^a}{T}\right)^l}. \quad (20)$$

We first look for equilibria where $T = 0$. In this case we see from equations (17) and (19) respectively that $D_{tumor} = E_{tumor}^a = 0$. From (11) we get that $D_{blood} = 0$ and from (14) that $D_{spleen} = 0$ (since we are only interested in those equilibria that lie in that part of the space where all the variables are non-negative). From equation (12) we have

$$E_{blood}^a = \frac{\mu_{SB}^{Normal}}{\mu_{BB}} E_{spleen}^a.$$

Substituting this into equation (15) we get

$$E_{spleen}^a = \frac{a_{E_a S} E_{naive}}{\mu_{SB}^{Normal} + a_{E_a S} + r_{am} - \frac{\mu_{BSE}}{\mu_{BB}} \mu_{SB}^{Normal}},$$

so

$$E_{blood}^a = \frac{\mu_{SB}^{Normal}}{\mu_{BB}} \left(\frac{a_{E_a S} E_{naive}}{\mu_{SB}^{Normal} + a_{E_a S} + r_{am} - \frac{\mu_{BSE}}{\mu_{BB}} \mu_{SB}^{Normal}} \right).$$

From equation (13) we see that

$$E_{blood}^m = \frac{\mu_{SB}^{Normal}}{\mu_{BB}} E_{spleen}^m.$$

Substituting this into equation (16) we get

$$E_{spleen}^m = \left(\frac{r_{am}}{a_{Em} + \mu_{SB}^{Normal} - \frac{\mu_{BSE}}{\mu_{BB}} \mu_{SB}^{Normal}} \right) \left(\frac{a_{E_a S} E_{naive}}{\mu_{SB}^{Normal} + a_{E_a S} + r_{am} - \frac{\mu_{BSE}}{\mu_{BB}} \mu_{SB}^{Normal}} \right),$$

so

$$E_{blood}^m = \frac{\mu_{SB}^{Normal}}{m\mu_{BB}} \left(\frac{r_{am}}{a_{Em} + \mu_{SB}^{Normal} - \frac{\mu_{BSE}}{\mu_{BB}} \mu_{SB}^{Normal}} \right) \left(\frac{a_{E_a S} E_{naive}}{\mu_{SB}^{Normal} + a_{E_a S} + r_{am} - \frac{\mu_{BSE}}{\mu_{BB}} \mu_{SB}^{Normal}} \right).$$

Thus, there exists a unique equilibrium with $T = 0$. We call this equilibrium T^* . When the parameters take on the values given Table 1 in the Appendix, it is the point:

$$\begin{aligned}
D_{blood} &= 0 & E_{spleen}^a &= 69.1191 & E_{tumor}^a &= 0 \\
D_{spleen} &= 0 & E_{blood}^m &= 0.1190 & T &= 0 \\
E_{blood}^a &= 6.2086 & E_{spleen}^m &= 1.3243 & D_{tumor} &= 0
\end{aligned}$$

To find the other equilibria, notice that the right-hand side of equation (20) is always a number between 0 and d . This means that the equation has a positive solution if and only if $\min\{0, k(1 - d/r)\} < T \leq k$. For any such T , this equation is satisfied when

$$E_{tumor}^a = \left(\frac{sr \left(1 - \frac{T}{k}\right)}{d - r \left(1 - \frac{T}{k}\right)} \right)^{1/l} T.$$

Substituting into equation (17) we see that it is satisfied if and only if

$$E_{blood}^a = \frac{(aE_a T + cT)(\alpha + T)}{\mu_{BB} T} \left(\frac{sr \left(1 - \frac{T}{k}\right)}{d - r \left(1 - \frac{T}{k}\right)} \right)^{1/l} T.$$

Similarly, equation (19) is satisfied if and only if

$$D_{tumor} = \left(\frac{mT}{q + T} \right) \left(\frac{1}{\mu_{TB} + a_D} \right)$$

and then equation (11) is satisfied if and only if

$$D_{blood} = \frac{m\mu_{TB}}{\mu_B} \left(\frac{mT}{q + T} \right) \left(\frac{1}{\mu_{TB} + a_D} \right).$$

Plugging these values back into equation (14), we obtain a quadratic equation from [2]:

$$\begin{aligned}
0 &= -\theta_{shut}(\mu_{SB}^* + \Delta\mu)M \\
&+ (\theta_{shut}\mu_{SB}^* a_D + \Delta\mu\theta_{shut} a_D + \theta_{shut} b_{DE} \mu_{BB} E_{blood}^a - \mu_{SB}^* M) D_{spleen} \\
&+ (\mu_{SB}^* + b_{DE} E_{blood}^a \mu_{BB})(D_{spleen})^2
\end{aligned}$$

where

$$M = MaxD \left(1 - e^{-\frac{\mu_{BS} D_{blood}}{MaxD}} \right).$$

The quadratic equation has the general form

$$ax^2 + bx + c = 0$$

where

$$\begin{aligned}
a &= \mu_{SB}^* + b_{DE} E_{blood}^a \mu_{BB} > 0 \\
b &= \theta_{shut}\mu_{SB}^* a_D + \Delta\mu\theta_{shut} a_D + \theta_{shut} b_{DE} \mu_{BB} E_{blood}^a - \mu_{SB}^* M > 0
\end{aligned}$$

and

$$c = -\theta_{shut}(\mu_{SB}^* + \Delta\mu) < 0.$$

Discriminant $\Delta = b^2 - 4ac > 0$, so this quadratic equation always yields two solutions, x_1 and x_2 . However,

$$x_1 x_2 = \frac{c}{a} < 0,$$

which means one solution is negative while the other is positive. We are only interested in the positive solution. From equation (16), we get a value for E_{spleen}^{m*} ,

$$E_{spleen}^{m*} = \frac{r_{am}E_{spleen}^{a*}}{a_{E_m} + b_a D_{spleen}^* + \mu_{SB}(D_{spleen}^*(1 - \mu_{BSE}/\mu_{BB}))}.$$

Lastly, equation (13) gives E_{blood}^{m*} in terms of E_{spleen}^{m*} ,

$$E_{blood}^{m*} = \frac{\mu_{BB}}{\mu_{SB}(D_{spleen}^*)} E_{blood}^{a*}.$$

This completes the computation of all equilibrium values in term of \tilde{T} . Notice that equation (15) is never used through the calculation. By plugging in all values we will obtain another equation of \tilde{T} . Although it is not clear how many solutions of \tilde{T} it will yield, simulation exclusively indicates there is only one equilibrium, meaning only one solution for \tilde{T} .

Recall that we are interested in those initial conditions for which $T \rightarrow 0$ as $t \rightarrow \infty$. We shall show in section 6 that every such solution actually converges to the equilibrium where $T = 0, T^*$, so it suffices to determine the basin of attraction of this equilibrium. Notice that at this equilibrium we have $T = E_{tumor}^a = 0$, so the second term in equation (18) is not differentiable. This means that we cannot linearize about this equilibrium and investigate its stability in the usual way. Our general approach is outlined in Section 4 below. However, there is one observation that we can make that doesn't require much machinery. This deals with the case when $d < r$ and is outlined in the theorem below.

Theorem 1. *If $d < r$, then T^* is unstable.*

Proof. Notice that

$$\begin{aligned} T' &= \left[r \left(1 - \frac{T}{k} \right) - d \frac{\left(\frac{E_{tumor}^a}{T} \right)^l}{s + \left(\frac{E_{tumor}^a}{T} \right)^l} \right] T \\ &\geq \left[r \left(1 - \frac{T}{k} \right) - d \right] T. \end{aligned}$$

Since $d < r$, $1 - \frac{d}{r} > 0$, and if $0 < T < k \left(1 - \frac{d}{r} \right)$, then

$$T' > \left[r \left(1 - \frac{k(1 - d/r)}{k} \right) - d \right] T = 0$$

so T is increasing. The result follows. \square

The proof of Theorem 1 actually works in the full system where $v_{tumor}(t)$ and $v_{blood}(t)$ may not be identically 0. In other words, when $d < r$, dendritic cell therapy cannot, by itself, kill off the tumor.

4 General Approach

The chart below shows which variables each of the other variables depends on. Notice that the first six variables, D_{blood} through E_{spleen}^m , form the blood and spleen compartments. They depend only on each other and one other variable, D_{tumor} . Similarly, the last three variables, E_{tumor}^a , T , and D_{tumor} form the tumor compartment. They depend only on each other and one other variable, E_{blood}^a .

	D_{blood}	D_{spleen}	E_{blood}^a	E_{spleen}^a	E_{spleen}^m	E_{spleen}^m	E_{tumor}^a	T	D_{tumor}
$\frac{d}{dt} D_{blood}$	✓								✓
$\frac{d}{dt} D_{spleen}$	✓	✓		✓					
$\frac{d}{dt} E_{blood}^a$		✓	✓	✓					
$\frac{d}{dt} E_{spleen}^a$		✓	✓	✓		✓			
$\frac{d}{dt} E_{blood}^m$		✓			✓	✓			
$\frac{d}{dt} E_{spleen}^m$		✓		✓	✓	✓			
$\frac{d}{dt} E_{tumor}^a$			✓				✓	✓	
$\frac{d}{dt} T$							✓		
$\frac{d}{dt} D_{tumor}$								✓	✓

Our approach is to study the behavior of the variables in the blood and spleen compartments where we treat D_{tumor} as an external function of time, and to study the three variables in the tumor compartment where we treat E_{blood}^a as an external function of time. Our hope is then to understand how these two subsystems feed into each other and thereby understand the solutions to the complete system of nine differential equations (11) through (19). We have had partial success to date.

5 The Blood and Spleen Compartments

In this section, we take a closer look at the blood and spleen compartments. We write the model out explicitly below for future reference.

$$\frac{d}{dt}D_{blood} = -\mu_B D_{blood} + \mu_{TB} D_{tumor}(t) \quad (21)$$

$$\frac{d}{dt}E_{blood}^a = \mu_{SB}(D_{spleen})E_{spleen}^a - \mu_{BB}E_{blood}^a \quad (22)$$

$$\frac{d}{dt}E_{blood}^m = \mu_{SB}(D_{spleen})E_{spleen}^m - \mu_{BB}E_{blood}^m \quad (23)$$

$$\frac{d}{dt}D_{spleen} = \left(MaxD \left(1 - e^{\left(\frac{-\mu_{BS}D_{blood}}{MaxD} \right)} \right) \right) - a_D D_{spleen} - b_{DE} E_{spleen}^a D_{spleen} \quad (24)$$

$$\begin{aligned} \frac{d}{dt}E_{spleen}^a &= \mu_{BSE}E_{blood}^a - \mu_{SB}(D_{spleen})E_{spleen}^a + b_a D_{spleen} E_{spleen}^m \\ &\quad + a_{EaS} E_{naive} - (a_{EaS} + r_{am}) E_{spleen}^a \\ &\quad + b_p \frac{D_{spleen}(t - \tau_D) E_{spleen}^a(t - \tau_D)}{\theta_D + D_{spleen}(t - \tau_D)} \end{aligned} \quad (25)$$

$$\begin{aligned} \frac{d}{dt}E_{spleen}^m &= r_{am} E_{spleen}^a - a_{Em} E_{spleen}^m + b_a D_{spleen} E_{spleen}^m + \mu_{SB}(D_{spleen}) E_{spleen}^m \\ &\quad + \mu_{BSE} E_{blood}^m \end{aligned} \quad (26)$$

Analysis of this system is difficult because of the delay, but we have some partial results. Figures 6 and 7 show typical simulations where D_{tumor} is constant. Notice that in both cases the solutions appear to converge to an equilibrium. In Figure 8 we zoom in on the solutions in 6. We can see that the solutions oscillate as we might expect because of the delay but they are at an amplitude that's very small compared to the global behavior.

Our first result about this system is Theorem 2 which concerns the boundedness of the solutions. We suspect that for any bounded function $D_{tumor}(t)$, the conclusion of the theorem is still valid and simulations appear to support this conjecture. Indeed, the model would not be physically reasonable if solutions became unbounded, but a proof of this is important in order to prove other results about the system. The proof in the case of a general bounded function $D_{tumor}(t)$ is elusive because we have to deal with the delay (in Theorem 2 we are able to bound the delay term). It is sufficient to determine boundedness of the solutions for functions $D_{tumor}(t)$ that are bounded because $D_{tumor}(t)$ is always bounded in the full 9-variable model (see Section 6).

Let $\alpha = \min\{\mu_{BB} - \mu_{BSE}, a_D, a_{EaS}, a_{Em}\}$. Also let

$$\beta = \frac{-\mu_{BS}\mu_B MaxD}{\alpha\mu_{TB}} \ln \left(1 - \frac{a_D\alpha}{4b_p MaxD} \right)$$

Note here that for parameter values in the appendix, $\frac{a_D\alpha}{4b_p MaxD} < 1$.

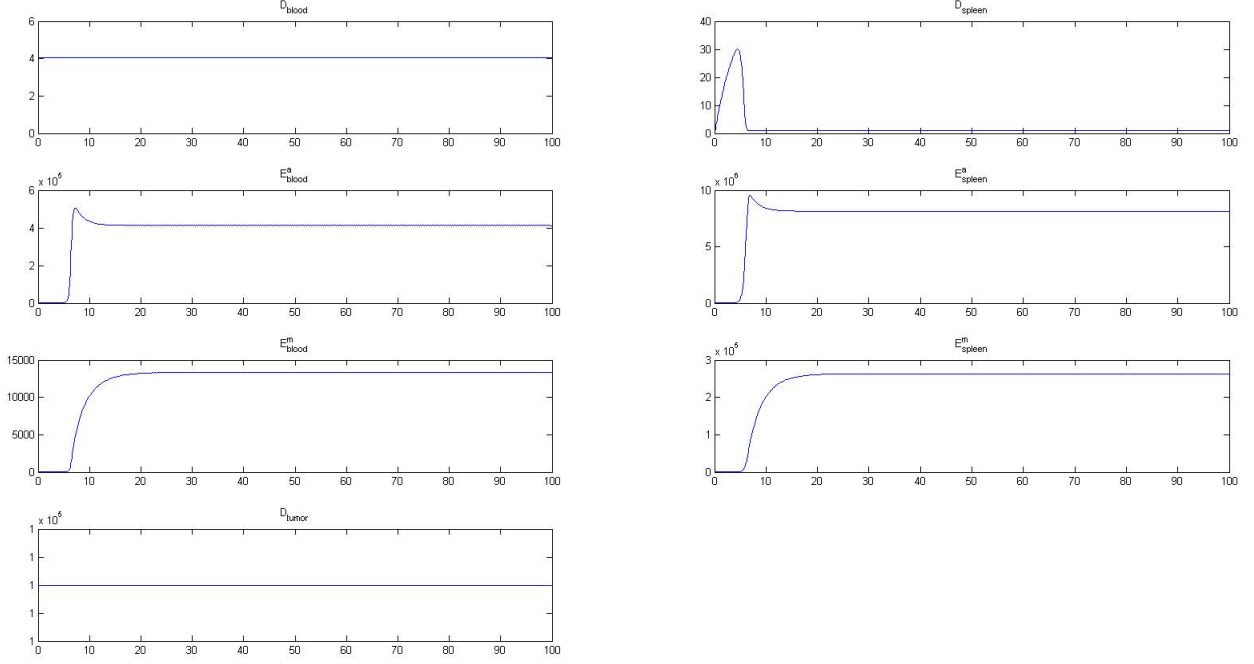


Figure 6: $D_{tumor} = 1 \times 10^5$

Theorem 2. *If $D_{tumor}(t) < \beta$ for all t then every solution to Equations (21) to (26) is bounded for all time.*

Proof. Note that $D'_{blood} < -\mu_B D_{blood} + \mu_{TBC}$, it follows that

$$D_{blood}(t) \leq D_{blood}(0)e^{-\mu_B t} + \frac{\mu_{TBC}}{\mu_B}(1 - e^{-\mu_B t}) \rightarrow \frac{\mu_{TBC}}{\mu_B}.$$

Choose time T_1 such that for all $t > T_1$,

$$D_{blood}(t) < \frac{2\mu_{TBC}}{\mu_B} = -MaxD \ln \left(1 - \frac{a_D \alpha}{4b_p MaxD} \right).$$

Now notice that

$$D'_{spleen} \leq MaxD \left(1 - e^{-\frac{\mu_{BS} D_{blood}}{MaxD}} \right) - a_D D_{spleen}.$$

But for all $t > T_1$,

$$\begin{aligned} MaxD \left(1 - e^{-\frac{\mu_{BS} D_{blood}}{MaxD}} \right) &< MaxD \left(1 - e^{-\frac{\mu_{BS} 2\mu_{TBC}}{MaxD \mu_B}} \right) \\ &= MaxD \left(\frac{a_D \alpha}{4b_p MaxD} \right) \\ &= \frac{a_D \alpha}{4b_p}, \end{aligned}$$

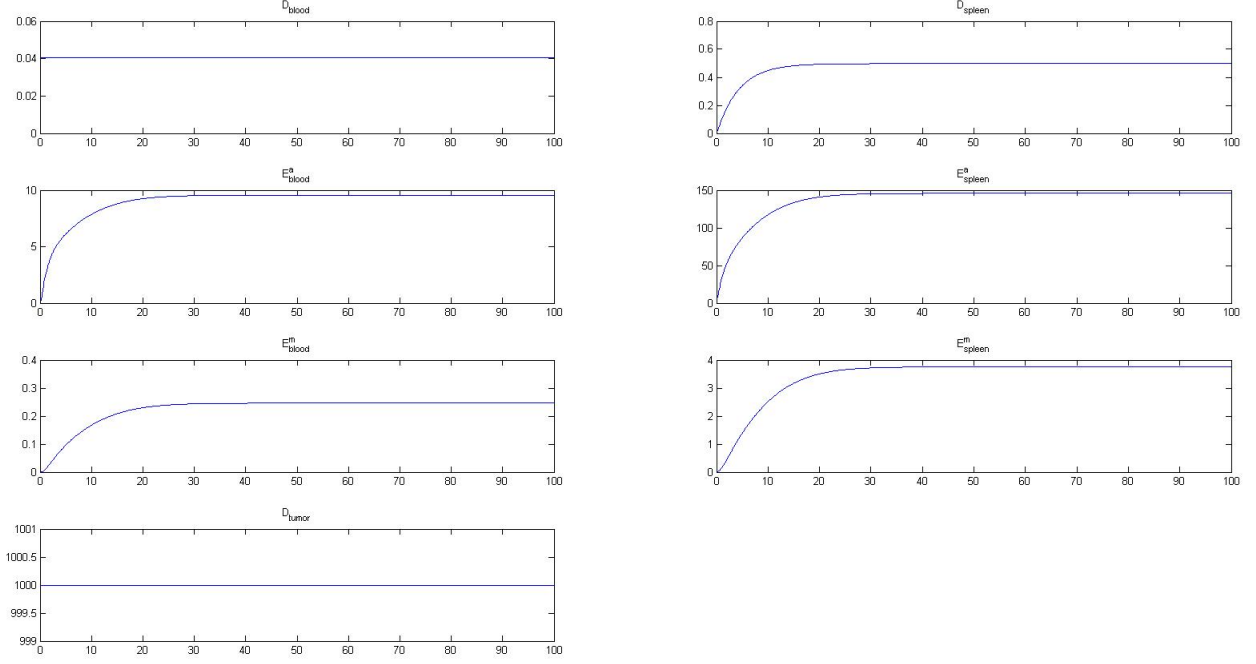


Figure 7: $D_{tumor} = 1 \times 10^3$

so

$$D'_{spleen} \leq \frac{a_D \alpha}{4b_p} - a_D D_{spleen}.$$

Thus, for all $t > T_1$,

$$D_{spleen}(t) \leq D_{spleen}(T_1) e^{-a_D(t-T_1)} + \frac{\alpha}{4b_p} \left(1 - e^{-a_D(t-T_1)}\right) \rightarrow \frac{\alpha}{4b_p}.$$

Choose $T_2 > T_1$ such that for all $t > T_2$,

$$D_{spleen}(t) < \frac{\alpha}{2b_p}.$$

Let $s = E_{blood}^a + E_{blood}^m + E_{spleen}^a + E_{spleen}^m$. Then for all $t > T_2 + \tau_D$,

$$\begin{aligned} s' &= -(\mu_{BB} + \mu_{BSE})(E_{blood}^a + E_{blood}^m) - a_{E_a S} E_{spleen}^a \\ &\quad - a_{E_m S} E_{spleen}^m - b_a D_{spleen} E_{spleen}^m + a_{E_a S} E_{naive} \\ &\quad + b_p \frac{D_{spleen}(t - \tau_D)}{\theta_D + D_{spleen}(t)} E_{spleen}^a(t - \tau_D) \\ &\leq -\alpha s + a_{E_a S} E_{naive} + \frac{\alpha}{2} E_{spleen}^a(t - \tau_D) \end{aligned}$$

Choose M such that:

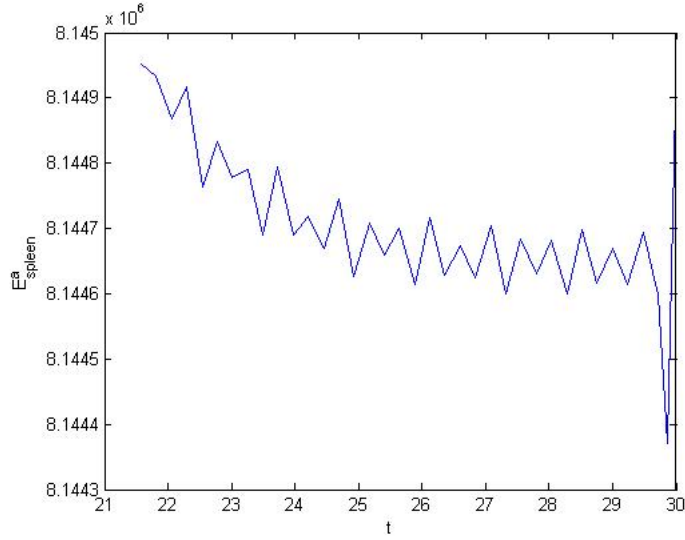


Figure 8: Closer look at E_{spleen}^a graph from fig. 6

- All the variables are less than M for $-\tau_D \leq t \leq T_2 + \tau_D$,
- $M > \frac{2a_{E_a}SE_{naive}}{\alpha}$.

We shall show that $s < M$ for all time. Suppose this is not the case. Let T_3 be the first time that $s = M$. By our choice of M , $T_3 > T_2 + \tau_D$ and since this is the first time that $s = M$, $E_{spleen}^a(T_3 - \tau_D) < M$. Thus

$$\begin{aligned} s'(T_3) &\leq -\alpha M + a_{E_a}SE_{naive} + \frac{\alpha}{2}M \\ &= -\frac{\alpha}{2}M + a_{E_a}SE_{naive} \\ &< 0. \end{aligned}$$

Thus there exists a time $T_4 < T_3$ such that $s(T_4) > M$, which means that there is a time $T_5 < T_4 < T_3$ at which $s(T_5) = M$. This is a contradiction to the definition of T_3 . It follows that $s < M$ for all time. \square

Our next result concerns the case when $D_{tumor}(t) \equiv 0$. In this case we have a complete understanding of the system. This case is interesting in its own right since it corresponds to the model of Ludewig *et al.*

Theorem 3. *The system defined by Equations (21) to (26) where $D_{tumor} \equiv 0$ has a unique equilibrium that is globally asymptotically stable.*

Proof. Setting the left-hand side of equations (11) through (16) equal to 0, it is easy to see that the system has a unique equilibrium. It follows from (11) that $D_{blood} \rightarrow 0$ exponentially as $t \rightarrow \infty$. Looking at equation (14), it is then clear that $D_{spleen} \rightarrow 0$ as $t \rightarrow \infty$.

Now, setting $D_{blood} = D_{spleen} = 0$, we study the system of the other four variables. Let $\vec{x} = (E_{blood}^a, E_{blood}^m, E_{spleen}^a, E_{spleen}^m)$. Notice that

$$\vec{x}' = a\vec{x} + \vec{b}$$

where

$$A = \begin{bmatrix} -\mu_{BB} & 0 & \mu_{SB}^{Normal} & 0 \\ 0 & -\mu_{BB} & 0 & \mu_{SB}^{Normal} \\ \mu_{BSE} & 0 & -\mu_{SB}^{Normal} - a_{EaS} - r_{am} & 0 \\ 0 & \mu_{BSE} & r_{am} & -a_{Em} - \mu_{SB}^{Normal} \end{bmatrix}$$

and

$$\vec{B} = \begin{bmatrix} 0 \\ 0 \\ a_{EaS}E_{naive} \\ 0 \end{bmatrix}$$

The eigenvalues of A are:

$$\lambda_{1,2} = \frac{1}{2} \left[-(\mu_{BB} + a_{Em} + \mu_{SB}^{Normal}) \pm \sqrt{(\mu_{SB}^{Normal} + a_{Em} - \mu_{BB})^2 + 4\mu_{SB}^{Normal}\mu_{BSE}} \right]$$

$$\lambda_{3,4} = \frac{1}{2} \left[-(r_{am} + a_{EaS} + \mu_{SB}^{Normal} + \mu_{BB}) \pm \sqrt{(r_{am} + a_{EaS} + \mu_{SB}^{Normal} - \mu_{BB})^2 + 4\mu_{SB}^{Normal}\mu_{BSE}} \right]$$

and when evaluated at the parameters in the appendix:

$$\begin{aligned} \lambda_1 &= -0.6418261 & \lambda_2 &= -0.5219278 \\ \lambda_3 &= -5.7000738 & \lambda_4 &= -5.7000721 \end{aligned}$$

These are all negative, therefore the equilibrium is globally asymptotically stable. □

Note: In the above proof, we set $D_{blood} = D_{spleen} = 0$, whereas in the 6x6 system, both variables are approaching 0. We believe the result is the same with this difference, but have not reached a satisfying proof as yet.

When D_{tumor} is constant (but possibly not 0) it isn't hard to see that the system described by Equations (11) to (19) still has a unique equilibrium and we suspect that this equilibrium is still globally asymptotically stable. Simulations support this conjecture but a proof remains elusive because of the delay term. The first step in proving that the equilibrium is globally asymptotically stable is to show that the solutions are bounded. Looking back at equation (11), when D_{tumor} is a constant, then (11) converges to a constant.

This means that D_{spleen} is bounded above. If we could bound E_{spleen}^a then it would follow that E_{blood}^a is bounded. When E_{spleen}^a is large, we can see from (14) that D_{spleen} will become smaller which means that the coefficient of the growth term in equation (15) becomes very small so E_{spleen}^a must decrease. However, to make this into a rigorous proof, we need a better understanding of the delay.

In order to help us understand the affect of the delay term in the system defined by equations (11)-(19) we have been looking at the general delay differential equation

$$x'(t) = -\alpha x(t) + \beta(t)x(t - \tau) + f(t).$$

We have some bounds on the growth rate of x when $f(t) \equiv 0$ and β is a constant, but we have not been able to apply these results to the model.

6 The Tumor Compartment

The system below models the behavior of the variables in the tumor compartment. For simplicity we denote E_{tumor}^a by x , T by y and D_{tumor} by z . The variable E_{blood}^a is external to the system; we think of it simply as a function of time. Our goal is to understand the behavior of the system whatever function of time E_{blood}^a may be. The parameters all have the values given in the appendix except we explore different values of d and r .

$$\frac{dx}{dt} = \mu_{BB} \frac{y}{1+y} E_{blood}^a(t) - a_{E_a T} x - cxy \quad (27)$$

$$\frac{dy}{dt} = ry \left(1 - \frac{y}{k}\right) - d \frac{\left(\frac{x}{y}\right)^{\frac{2}{3}}}{s + \left(\frac{x}{y}\right)^{\frac{2}{3}}} y \quad (28)$$

$$\frac{dz}{dt} = \frac{my}{q+y} - (\mu_{TB} + a_D)z \quad (29)$$

Notice that x and y only depend on each other and not on z . This permits us to study the 2-variable system consisting of x and y alone. Having understood these solutions we then study the behavior of z . The system in x and y is particularly interesting because it contains the term $\frac{d\left(\frac{x}{y}\right)^{\frac{2}{3}}}{s + \left(\frac{x}{y}\right)^{\frac{2}{3}}}$ that is not differentiable at the origin.

6.1 The Two-Variable System in x and y Alone

We start by considering the case when $E_{blood}^a(t) = E_{blood}^a$ is constant. Figures 9, 10, and 11, show typical simulations in this case.

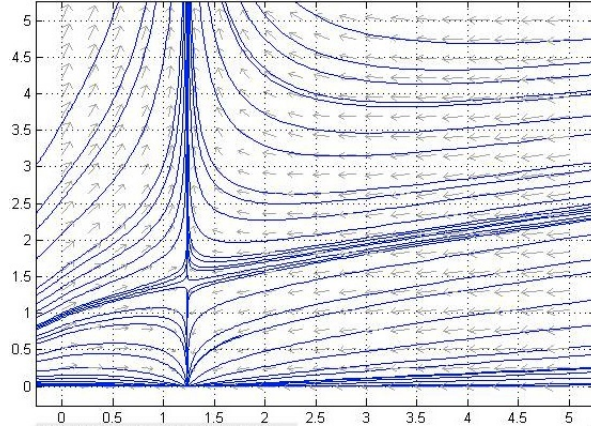


Figure 9: $d > r$, $E_{blood}^a = 1000$ (axis scale: $\times 10^4$)

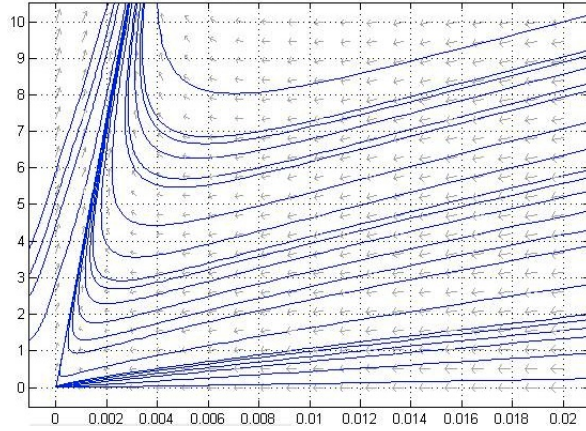


Figure 10: $d > r$, $E_{blood}^a = 0.03$

Notice that the origin $(0, 0)$ is always an equilibrium of the system. The system does not look locally linear near the origin because of the non-differentiable term. For some values of E_{blood}^a , d and r , the origin is unstable, for others it is semi-stable, and for yet others it is unstable. We shall see that there is always another stable equilibrium where y is large (near the carrying capacity of the tumor). Sometimes there is a third unstable equilibrium. The third equilibrium is helpful in determining the basin of attraction of the origin. In what follows we do a null-cline analysis of the system in order to quantify and provide proofs of these observations.

A simple calculation shows that the x-nullcline is given by:

$$x = \mu_{BB} E_{blood}^a \frac{y}{(1+y)(a_{E_a T} + cy)}.$$

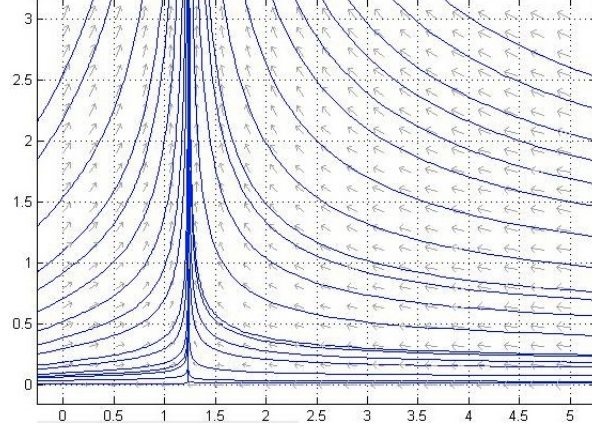


Figure 11: $d < r$, $E_{blood}^a = 1000$ (axis scale: $\times 10^4$)

The x-axis ($y = 0$) forms part of the y-nullcline. The other part is given by:

$$r \left(1 - \frac{y}{k}\right) = d \frac{\left(\frac{x}{y}\right)^{\frac{2}{3}}}{s + \left(\frac{x}{y}\right)^{\frac{2}{3}}}$$

$$\left(1 - \frac{y}{k}\right) \left[s + \left(\frac{x}{y}\right)^{\frac{2}{3}} \right] = \frac{d}{r} \left(\frac{x}{y}\right)^{\frac{2}{3}}$$

$$s \left(1 - \frac{y}{k}\right) + \left(\frac{x}{y}\right)^{\frac{2}{3}} - \frac{y}{k} \left(\frac{x}{y}\right)^{\frac{2}{3}} = \frac{d}{r} \left(\frac{x}{y}\right)^{\frac{2}{3}}$$

$$\left(\frac{x}{y}\right)^{\frac{2}{3}} = \left[\frac{s(1 - \frac{y}{k})}{\frac{d}{r} - (1 - \frac{y}{k})} \right]$$

$$x = \left[\frac{s(1 - \frac{y}{k})}{\frac{d}{r} - (1 - \frac{y}{k})} \right]^{\frac{3}{2}} y$$

The graph in Figure 12 shows the nullclines when $E_{blood}^a = 4.5 \times 10^5$, and $d = 1.25$.

Let

$$f(y) = \frac{\mu_{BB} E_{blood}^a}{1 + y}$$

and

$$g(y) = (a_{E_a T} + cy) \left[\frac{s(1 - \frac{y}{k})}{\frac{d}{r} - (1 - \frac{y}{k})} \right]^{\frac{3}{2}}$$

We have already observed that the origin is always an equilibrium. A point (x, y) is another equilibrium if and only if

$$x = \frac{\mu_{BB} E_{blood}^a}{(1 + y)(a_{E_a T} + cy)}$$

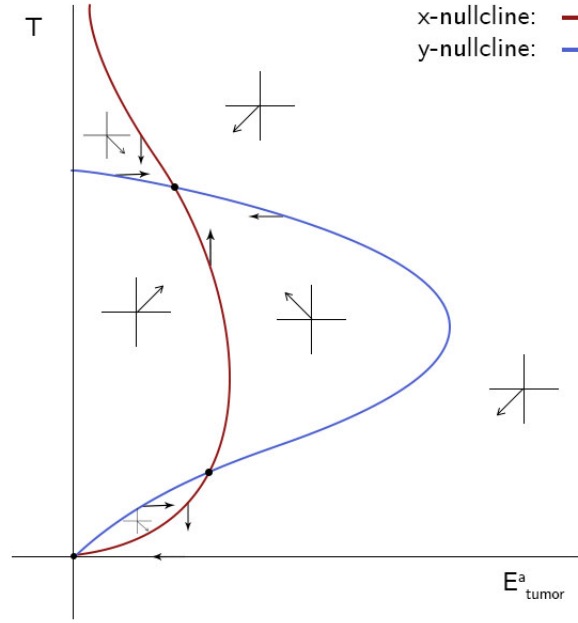


Figure 12: $E_{blood}^a > \left(\frac{s}{\frac{d}{r} - 1}\right)^{\frac{3}{2}} \frac{a_{E_a T}}{\mu_{BB}}$, $d > r$

and $f(y) = g(y)$. The graphs of f and g are shown in figures 13, 14, and 15 for three different sets of values of E_{blood}^a , d and r .

Observation 1: Consider the equilibria of the system defined by Equations (27) through (28).

- 1) If $d \leq r$, the equilibria consist of the origin and exactly one other point.
- 2) If $d > r$ and

$$E_{blood}^a \leq \left(\frac{s}{\frac{d}{r} - 1}\right)^{\frac{3}{2}} \frac{a_{E_a T}}{\mu_{BB}},$$

then the equilibria of the system consist of the origin and exactly one other point.

- 3) If $d > r$ and

$$E_{blood}^a > \left(\frac{s}{\frac{d}{r} - 1}\right)^{\frac{3}{2}} \frac{a_{E_a T}}{\mu_{BB}},$$

then the equilibria consist of the origin and exactly two other points.

We see this as follows:

Function f is defined, decreasing for all $y \geq 0$, and does not depend on E_{blood}^a . It decreases at an extremely high rate until some y that is relatively small compared to k . It

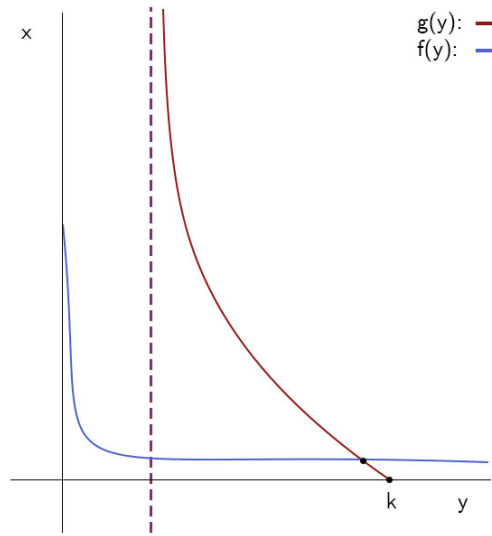


Figure 13: $d \leq r$

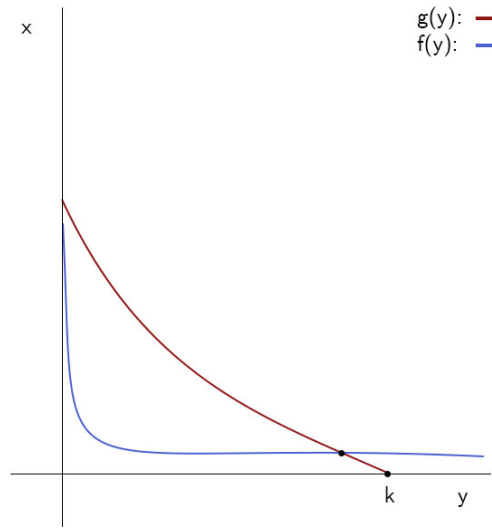


Figure 14: $d > r, E_{blood}^a \leq \left(\frac{s}{d-r-1}\right)^{\frac{3}{2}} \frac{aE_a T}{\mu_{BB}}$

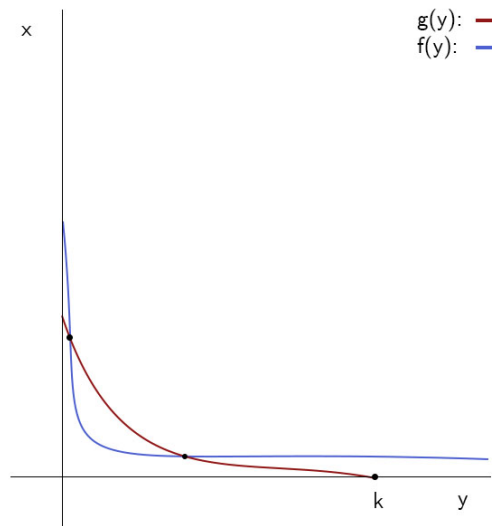


Figure 15: $d > r, E_{blood}^a > \left(\frac{s}{d-r-1}\right)^{\frac{3}{2}} \frac{aE_a T}{\mu_{BB}}$

then flattens and goes to 0 as y goes to infinity. The function g is also decreasing, though its rate of decrease is closer to a constant than that of f (see figures 13 through 15). Moreover, $g(k) = 0$.

1) When $d < r$, the function g is only defined for $k(1 - \frac{d}{r}) < y \leq k$ and has an asymptote at $y = k(1 - \frac{d}{r})$. In this case, there is only one intersection between f and g .

2) When $d > r$, g is still decreasing but now is defined for all $0 \leq y \leq k$ and

$$g(0) = a_{E_a T} \left(\frac{s}{\frac{d}{r} - 1} \right)^{\frac{3}{2}}.$$

By the inequality in the hypothesis we see that $g(0) \geq f(0)$. It follows that $f(y)$ intersects $g(y)$ only once.

3) In this case g is decreasing and defined for all $0 \leq y \leq k$ and

$$g(0) = a_{E_a T} \left(\frac{s}{\frac{d}{r} - 1} \right)^{\frac{3}{2}}$$

as in the second case above. This time, however, from the inequality in the hypothesis it follows that $f(0) > g(0)$. As f descends quickly it crosses the graph of g once, then it intersects g again when it flattens out.

Observation 2: Every solution to the system defined by equations (27) to (28) converges to some equilibrium. We divide the discussion into three cases.

Case I: $d \leq r$

Figure 16 shows a sketch of the nullclines and the direction fields in all regions in this case.

All solutions go to equilibrium point I, except those that lie on the line $T = 0$, which go to the origin.

Case II: $d > r$ and $E_{blood}^a \leq \left(\frac{s}{\frac{d}{r} - 1} \right) \frac{a_{E_a T}}{\mu_{BB}}$

Figure 17 shows a sketch of the nullclines and the direction fields in all regions in this case.

Everything in regions 1, 3 and 4 goes to equilibrium I. Points in the top left of region 2 enter region 1 and also go to equilibrium I. Points in the top right can go directly to equilibrium I. Points lower down can enter region 4 and be sent to equilibrium I. Points further down can just keep moving southeast without ever hitting the y-nullcline and converge to the origin.

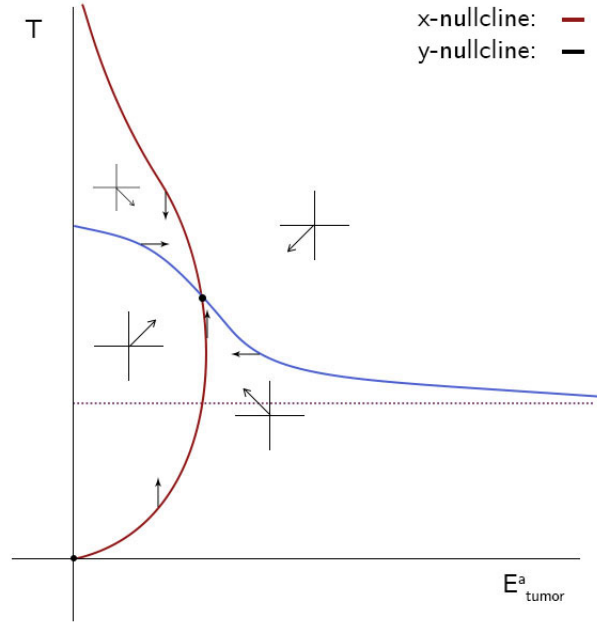


Figure 16: The graph of the two nullclines when $d \leq r$

It is not clear from the figure that these points exist, but simulations (see for example Figure 10) suggest that there are always such points. Only points on the E^a_{tumor} axis go to the origin.

$$\text{Case III: } d > r \text{ and } E^a_{blood} > \left(\frac{s}{\frac{d}{r} - 1} \right) \frac{aE_a T}{\mu_{BB}}.$$

Figure 18 shows a sketch of the nullclines and the direction fields in all regions in this case.

The nullclines define 5 different regions in phase space. Everything in region 1 goes to equilibrium I. Everything in 4 and top half of 3 also goes to equilibrium I. In the top left of region 2, points go into region 1 and be sent to equilibrium I. In top right of region 2, points can go directly to equilibrium I. Points lower down can enter region 4 and go to equilibrium I. Points even lower down in region 2 go to the origin. Everything in region 5 enters the bottom part of region 2. In the bottom part of region 3, points can hit the y-nullcline and enter region 5, and eventually go to the origin.

Of particular interest to us is the basin of attraction of the origin. We saw in the observations above that when $d \leq r$ the only solutions that converge to the origin are those where $T = 0$. When $d > r$ and

$$E^a_{blood} \leq \left(\frac{s}{\frac{d}{r} - 1} \right) \frac{aE_a T}{\mu_{BB}}$$

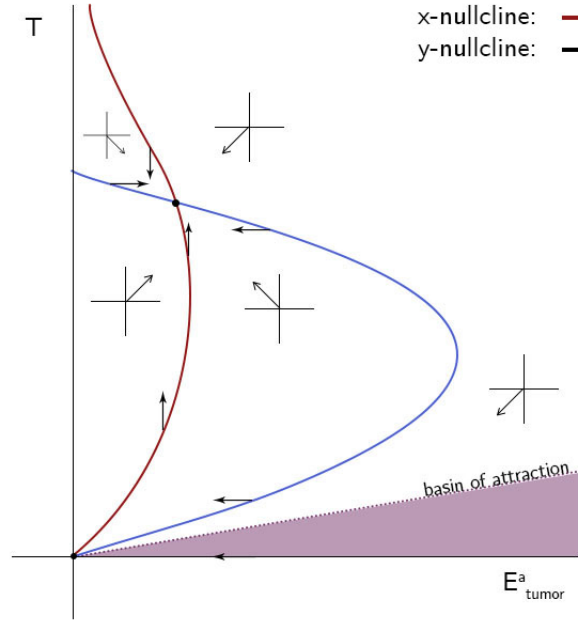


Figure 17: The graph of the two nullclines with $d > r$ and $E_{blood}^a \leq \left(\frac{s}{\frac{d}{r}-1}\right) \frac{aE_a T}{\mu_{BB}}$. Regions are labelled 1-4

we see numerically that points that lie in a sliver where T is small compared to E_{tumor}^a are in the basin of attraction of the origin but we haven't been able to prove this rigorously or locate this sliver more precisely (see the shaded region in Figure ??). When $d > r$ and

$$E_{blood}^a > \left(\frac{s}{\frac{d}{r}-1}\right) \frac{aE_a T}{\mu_{BB}}$$

there exists a third equilibrium that can help us identify the basin of attraction of the origin. Consider the shaded region that consists of part of region 3, all of region 5 and part of region 2. All the points in this region lie in the basin of attraction of the origin. We see this as follows. The part in region 2 consists of all points that lie vertically below equilibrium II. Notice that this part of the shaded region is invariant under the flow, so therefore all solutions go to the origin. There are also some points outside the shaded part of region 2 that lie in the basin of attraction of the origin, but we are not able to identify them precisely. Everything in region 5 enters the shaded part of region 2 and goes to the origin. The points in the shaded part of region 3 enter region 5 and go to the origin.

Because we are especially interested in the initial condition where $y > 0$ and $x = 0$, it is helpful to estimate how far the shaded area in region 3 extends. Let $(0, T_0)$ be the point in the phase plane where any solution passing through $(0, T)$ where $T < T_0$ converges to the origin and any solution passing through $(0, T)$ where $T > T_0$ converges to the other stable equilibrium. The charts below show the values of T_0 for different values of E_{blood}^a and d .

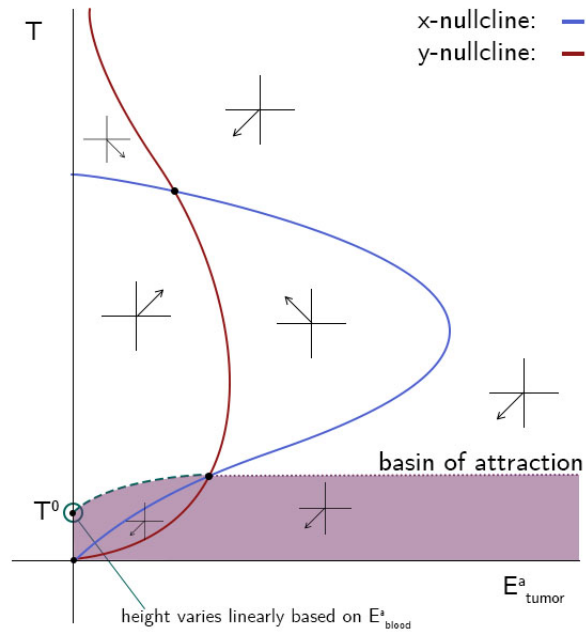


Figure 18: The graph of the two nullclines when $d > r$ and $E_{blood}^a > \left(\frac{s}{d-r-1}\right) \frac{aE_a T}{\mu_{BB}}$. Regions are labelled 1 - 5.

Parameter r has value 0.3954.
 $d = 1$

y_0	E_a^{blood}
0.2437	0.1
1.1612	0.2
2.0993	0.3
3.0419	0.4
3.9860	0.5
4.9292	0.6
5.8760	0.7
6.8212	0.8
7.7664	0.9
8.7127	1.0

$$E_{blood}^a = 1$$

y_0	d
2.8404	0.7
4.6075	0.8
6.5711	0.9
8.7127	1.0
11.0186	1.1
13.4778	1.2
16.082	1.3
18.8217	1.4
21.6908	1.5
24.6922	1.6

Polynomial approximation reveals a strong linear relationship between y_0 and E_{blood}^a . It is well-approximated by the function:

$$y_0 = 9.4520E_{blood}^a - 0.7200.$$

The coefficient of determination is 1 and it gives great predication of y_0 in larger scale. Locally, the relationship between y_0 and d can be best approximated by the following quadratic function with coefficient of determination 1:

$$y_0 = 7.5870d^2 + 6.9177d - 5.7636.$$

Unfortunately, it only offers a relatively accurate approximation for small values of d and results in huge errors on a larger scale. Overall, we are able to numerically determine the value of y_0 with

$$T_0 = 0.1145(7.8570d^2 + 6.9177d - 5.7636)(9.4250E_{blood}^a - 0.7200)$$

6.2 The Variable z

We have shown above that when E_{blood}^a is constant, along all solution curve for equation (27) and (28), y must converge some constant, y^* . Thus,

$$\frac{d}{dt}D_{tumor} = m(t) - (\mu_{TB} + a_D)D_{tumor}$$

where

$$m(t) \rightarrow m^* = \frac{my^*}{q + y^*} \quad as \quad y \rightarrow y^*.$$

As $m(t)$ is converging to a constant, D_{tumor} will also converges to a constant, namely $\frac{m^*}{\mu_{TB} + a_D}$. This concides with our observation that D_{tumor} always converge to a constant in any simulations.

6.3 3×3 discussion

We have determined the x,y-nullclines for equation (27) and (28) previously. When E_{blood}^a increases, the y-nullcline remains unchanged and the x-nullcline is stretched in the x-direction. This causes the equilibrium to move up-right along the y-nullcline and away from the origin. This will indeed increase the area of basin of attraction we identified earlier, which is bounded by y-nullcline and the horizontal ray starting from equilibrium to the right.

As for the part of basin attraction that lays above the y-nullcline, we could not elaborate the effect of increasing E_{blood}^a due to the lack of an explicit expression of the boundary. Nonetheless, we know that T_0 will move upwards along y-axis because of its linear dependency on E_{blood}^a . Moreover, for every appropriate E_{blood}^a , we will always have a unique solution that goes into its unstable equilibrium, appearing as the boundary of basin of attraction. If E_{blood}^a increases, all vectors in the field will have a smaller slope, due to a larger x-component. It follows that the solution going into the new unstable equilibrium will lay above the old one, resulting in an expansion of basin of attraction.

This interprets the phenomena that a solution growing towards the carrying-capacity equilibrium will occasionally be deflected half-way and pulled back into the origin equilibrium. In this case, the expansion of basin of attraction due to increasing E_{blood}^a is rapid enough to catch up with the growth of tumor.

7 Conclusion/Future Work

Thus far, we have been able to prove the stability of the blood and spleen compartment with respect to Ludewig's model in the 6×6 system analysis. However, in the blood and spleen compartment, $D_{tumor}(t)$ is not constant in general, and we are moving towards proving the boundedness of the six variables in that system, which will bring us closer to the general stability of that system. As we mentioned before, our reasoning tells us that the blood and spleen compartment is globally asymptotically stable given a constant number of dendritic cells in the tumor.

In the tumor compartment, we have been able to conduct nullcline analysis in order to determine the basin of attraction of the equilibrium at T^* , so as to put the patient into a situation where they can kill off tumor cells on their own, without any dendritic cell vaccinations.

In our future work, we would like further our understanding of the stability of the T^* equilibrium. Ultimately, we would like to determine the DC injections that will put the patient into the basin of attraction at the T^* equilibrium. We would also like to determine which parameters have the greatest effect on the basin of attraction of T^* , since we do not expect all patients to have the same parameter values.

Acknowledgments:

The authors would like to thank Andrea Bertozzi for organizing the 2012 summer Research Experience for Undergraduates at UCLA. The authors were supported by the California Research Training Program in Computational and Applied Mathematics through the NSF grant DMS-1045536.

A Parameter Values

The parameters used in the model are described in the following table. These parameter values are taken from DePillis *et al.*

Table 1: Parameter Values

Parameter name	Description	Value	Units
α	Component of μ_{BTE}	1	cell
μ_{BS}	Transfer rate of DCs from the blood to spleen	2.832	1/day
μ_B	Rate of DC emigration from blood	27.072	1/day
$\tilde{\mu}_{BB}$	Total elimination rate of CTL from blood	5.8	1/day
μ_{BB}	Scaled and shifted elimination rate of CTL from blood	Calculated	1/day
μ_{SB}^{Normal}	Normal DC transfer rate from spleen to blood	0.5120	1/day
μ_{SB}^*	DC reduced transfer rate from spleen to blood	0.012	1/day
$\tilde{\mu}_{BSE}$	Transfer rate of activated CTLs from blood to spleen	0.022	1/day
$\mu_{BSE} = \tilde{\mu}_{BSE}Q_{spleen}/Q_{blood}$	Scaled transfer rate of activated CTLs from blood to spleen	Calculated	1/day
μ_{LB}	Transfer rate of DCs from the liver to the blood	0.51	1/day
μ_{BL}	Transfer rate of DCs from the blood to the liver	0.1	1/day
$\mu_{BTE} = \mu_{BB}(T)$	T-dependent rate at which effector cells enter the tumor compartment from the blood	Calculated	1/day
μ_{TB}	Rate of transfer of DC from tumor to blood	0.0011	1/day
Q_{blood}	Murine blood volume	3	ml
Q_{spleen}	Murine spleen volume	0.1	ml
Q_{liver}	Murine liver volume	0.5	ml
a_D	Natural death rate of DCs in the spleen	0.2310	1/day

Parameter name	Description	Value	Units
\tilde{b}_{DE}	Elimination rate of DCs by activated CTLs (per concentration)	0.13×10^{-6}	1/cell·day
$b_{DE} = \tilde{b}_{DE}/Q_{spleen}$	Per cell elimination rate of DCs by activated CTLs	Calculated	1/day
a_{EaS}	Natural death rate of activated CTLs in spleen	0.1199	1/day
E_{naive}	Number of naive CTL cells contributing to primary clonal expansion	370	cells
b_p	Maximal expansion factor of activated CTL	85	1/day
τ_D	Duration of pre-programmed CTL divisions	0.5	days
$\tilde{\theta}_D$	Threshold in DC density in the spleen for half maximal proliferation rate of CTL	2.12×10^3	cell/ml
$\theta_D = \tilde{\theta}_D Q_{spleen}$	Scaled threshold in DC density in the spleen for half maximal proliferation rate of CTL	Calculated	cell
r_{am}	Reversion rate of activated CTL to memory CTL	0.01	1/day
\tilde{b}_a	Activation rate of memory CTL concentration by DCs	1×10^{-3}	ml/(cell·day)
$b_a = \tilde{b}_a/Q_{spleen}$	Per cell activation rate of memory CTLs by DCs	Calculated	1/(cell·day)
a_{Em}	Natural death rate of memory CTLs in the spleen	0.01	1/day
$\tilde{\theta}_{shut}$	Threshold in DC density in the spleen for half maximal transfer rate from spleen to blood	13	cells/ml
$\theta_{shut} = \tilde{\theta}_{shut} Q_{spleen}$	Scaled threshold in DC density in the spleen for half maximal transfer rate from spleen to blood	Calculated	cells

Parameter name	Description	Value	Units
$a_{E_a T}$	Natural death rate of activated CTLs in tumor compartment	$\log(2)/1.5$	1/day
r	Tumor growth rate	0.3954	1/day
k	Carrying capacity of tumor	1×10^9	cells
c	Rate at which activated CTLs are inactivated by tumor cells	9.42×10^{-12}	1/(cell·day)
d	Steepness coefficient of the fractional tumor kill by CTLs	0.35	1/day
s	Value of \mathcal{D} necessary for half maximal activated CTL toxicity	1.4	unitless
l	Immune strength scaling exponent	2/3	unitless
m	Steepness coefficient of native immune response	2.4388×10^4	cells/ml
q	Value of T necessary for half maximal native immune response	100	cells

B Equilibrium Values

Here are the approximate values of the equilibrium points for varying values for E_{blood}^a and d in the 2×2 system analysis. Besides the equilibrium at T^* (from which we recall is at $T = 0$), we have two other equilibria, namely the intermediate equilibrium (near the origin), and the equilibrium near k (carrying capacity).

Note: When $d \leq r$, then the equilibrium at T^* is unstable.

Table 2: Equilibrium points where $d = 0.35$.

E_{blood}^a	Intermediate Equilibrium	Equilibrium Near k
0	none	(0.0000, 999999996.5474)
10	none	(120.8857, 999984541.9986)
5×10	none	(604.4288, 999954801.4699)
5×10^2	none	(6044.3076, 999790222.5286)
5×10^3	none	(60443.9985, 999026633.7926)
5×10^4	none	(604482.7042, 995489242.8098)
5×10^5	none	(6046792.8012, 979218224.5963)

Table 3: Equilibrium points where $d = r = 0.3954$.

E_{blood}^a	Intermediate Equilibrium	Equilibrium Near k
0	none	(0.0000, 1000000000.0192)
10	(0.0017, 0.0000)	(120.8857, 999982537.2983)
5×10	(0.0038, 0.0000)	(604.4288, 999948938.0730)
5×10^2	(1.5222, 0.0000)	(6044.3109, 999763007.0023)
5×10^3	(0.0219, 0.0000)	(60444.1511, 998900279.9506)
5×10^4	none	(604489.7922, 994902097.2654)
5×10^5	(3.2095, 0.0000)	(6047123.8851, 976478836.0816)

Table 4: Equilibrium points where $d = 0.85$.

E_{blood}^a	Intermediate Equilibrium	Equilibrium Near k
0	none	(0.0000, 1000000002.5708)
10	(122.0442, 91.4431)	(120.8857, 999962457.9691)
5×10	(615.3931, 455.5314)	(604.4296, 999890227.2826)
5×10^2	(6166.1521, 4589.1097)	(6044.3438, 999490436.5067)
5×10^3	(61673.5608, 45904.1797)	(60445.6804, 997633869.7193)
5×10^4	(616742.5017, 459579.6325)	(604561.1434, 988996710.8838)
5×10^5	(6166910.3406, 4649755.4876)	(6050513.5566, 948449655.0488)

References

- [1] van den Driessche P. Zou X. Cooke, K. Interaction of maturation delay and nonlinear birth in population and epidemic models. *Journal of Mathematical Biology*, 39(4):332–352, 1999.
- [2] Lisette dePillis, Angela Gallegos, Amy Radunskaya, Chris DeBoever, Helen Wu, and Megan Hunter. A model of dendritic cell therapy for melanoma. 2009.
- [3] A. Gallegos and A. Radunskaya. Do Longer Delays Matter? The Effect of Prolonging Delay in CTL Activation. *ArXiv e-prints*, July 2010.
- [4] Sang Bae Han, Se Hyung Park, Young Jin Jeon, Young Kook Kim, Hwan Mook Kim, and Kyu Hwan Yang. Prodigiosin blocks t cell activation by inhibiting interleukin-2r expression and delays progression of autoimmune diabetes and collagen-induced arthritis. *Journal of Pharmacology and Experimental Therapeutics*, 299(2):415–425, 2001.
- [5] Tae-Hyung Lee, Young-Hun Cho, and Min-Geol Lee. Larger numbers of immature dendritic cells augment an anti-tumor effect against established murine melanoma cells. *Biotechnology Letters*, 29:351–357, 2007. 10.1007/s10529-006-9260-y.
- [6] Burkhard Ludewig, Philippe Krebs, Tobias Junt, Helen Metters, NevilleJ. Ford, RoyM. Anderson, and Gennady Bocharov. Determining control parameters for dendritic cell-cytotoxic t lymphocyte interaction. *European Journal of Immunology*, 34(9):2407–2418, 2004.

Table 5: Equilibrium points where $d = 1.00$.

E_{blood}^a	Intermediate Equilibrium	Equilibrium Near k
0	none	(0.0000, 1000000000.4631)
10	(122.4610, 139.0956)	(120.8858, 999955833.7518)
5×10	(615.8694, 701.1603)	(604.4298, 999870855.1582)
5×10^2	(6166.6193, 7039.0341)	(6044.3547, 999400476.8668)
5×10^3	(61674.0001, 70410.8931)	(60446.1857, 997215524.0850)
5×10^4	(616739.8815, 705208.4381)	(604584.7640, 987037582.7879)
5×10^5	(6166594.6297, 7165239.4185)	(6051663.7190, 938946310.6758)

Table 6: Equilibrium points where $d = 1.25$.

E_{blood}^a	Intermediate Equilibrium	Equilibrium Near k
0	none	(0.0000, 1000000000.6057)
10	(122.8246, 235.1169)	(120.8858, 999944790.7541)
5×10	(616.2246, 1179.8190)	(604.4302, 999838563.9501)
5×10^2	(6166.9718, 11818.2706)	(6044.3728, 999250519.6614)
5×10^3	(61674.2766, 118341.1924)	(60447.0283, 996517749.9759)
5×10^4	(616733.8091, 1186114.5687)	(604624.4070, 983760492.9437)
5×10^5	(6165968.7416, 12148214.1531)	(6053618.8166, 922800745.4050)

- [7] Olivier Preynat-Seauve, Emmanuel Contassot, Prisca Schuler, Lars E French, and Bertrand Huard. Melanoma-infiltrating dendritic cells induce protective antitumor responses mediated by t cells. *Melanoma Research*, 17(3):169–176, 2007.